Solving the landing problem of hopping robots: the elastic cage design

Paolo Fiorini, Francesco Bovo e Lorenzo Bertelli
Department of Computer Science
University of Verona
Strada le Grazie, 15 -- 37134 Verona, Italy
Email: paolo.fiorini@.univr.it

Mircea Gh. Munteanu
Dipartimento di Ingegneria Elettrica, Gestionale
e Meccanica (DIEGM)
Università degli Studi di Udine
munteanu@uniud.it

INTRODUCTION

This paper discusses one of the main challenges of planetary mobility by hopping, namely the need to ensure safe and repeatable landing in the adverse conditions of planetary surface. The problem in fact, is rather complex, since it does not only involve the physical survival of the device on landing, but also its weight, the complexity of the mechanisms on board, the design of specific energy reservoirs, and the duration and reliability of a possible mission. In other words, the landing strategy and its ancillary equipment are the key issues in the design of a hopping robot for the exploration of unknown terrain over an extended period of time.

Two main reasons are given to justify the research in hopping robots. The first is that smaller planetary rovers would allow space missions to small planetary bodies, characterized by low to medium gravitational environments. This approach in fact was actually followed by the recent Hayabusa mission of the Japanese Space Agency Jaxa aimed at the exploration of asteroid Itokawa by means of a small hopping robot. The second justification of studying small hopping robots lies in the possibility of flanking the large exploration rovers with a fleet of small devices, equipped with high mobility and maneuverability to act as scouts and sensors of the large rover. So far, all successful missions to Mars have focused on the single (or multiple, but treated independently) vehicle paradigm, i.e. the 6-wheeled rover, as seen in the Pathfinder mission's Sojourner vehicle [1]. Because of its unique rocker-bogey suspension, a 6-wheeled rover of the Sojourner type can traverse obstacles that are about 1.5 times the vehicle's wheel diameter. However, this still represents only a fraction of the vehicle's overall body length and it imposes severe limitations on the obstacle size, compared to body length that can be overcome. Furthermore, small-wheeled rovers, such as the Jet Propulsion Laboratory – NASA *nano-rover* [2], can only go over obstacles a few cm in height, because of the limitations imposed by wheels. Legged robots can overcome the limited traversability of wheeled vehicles in many rugged terrains [3], and they have previously been proposed for Lunar and Martian exploration [4], and demonstrated in an Alaskan volcano [5]. However, their mechanical complexity and weak reliability has never made them viable options for planetary exploration platforms. Thus, small size robots endowed with an excellent mobility, such as jumping robots, would help overcome obstacles and provide enough speed to carry out useful exploration missions. However, the main objection to this approach is the risk of sustaining irreparable damages at landing. Thus, much effort in the last years has gone into the design and analysis of different landing strategies. The last approach being currently studied consists of an elastic cage, which would provide both propulsion and protection to the rover.

To describe our initial design and simulations, we organize the paper as following. After summarizing relevant prior work below, including the various generations of NASA hopping robots, we discuss our new approach to hopping propulsion and landing protection. Because of the difficulty of the theoretical analysis of the system, the results presented are still preliminary, but they indicate the very good potential of the proposed design. To conclude, we summarize the main aspects of our research on hopping mobility and present our plans for future research in this area.

PRIOR WORK ON HOPPING ROBOTS

Hopping systems for planetary mobility were first proposed in [6], [7] as a promising transportation concept for astronauts in a Lunar environment. A first order analysis of Lunar hopper performance is presented in Ref. [8]. Based on data from the Apollo missions, the authors conclude that hopping can be an efficient form of transportation in a low-gravity environment. A hopping robot, whose structure is the precursor for some aspects of NASA-JPL first generation device, is described in [9]. The fabrication and testing of the prototype of a gas propeller for a Mars hopper has been described in [10], potentially capable of hops of several thousand meters. A second hopping system is described in [11], and is powered by an internal combustion chamber with steering achieved by rotating an off-centre mass. The common characteristic of these, and of the hopping systems described in this paper, is motion discontinuity, since a pause for re-orientation and recharge of the thrust mechanism is inserted between jumps. This is different from the motion paradigm of the most common hopping devices, which move without pauses between jumps [5], [11], [12], [13], [14]. The "scout" robot developed at the University of Minnesota [15] is a small two wheeled vehicle containing a leaf spring whose deployment can cause the scout to leap a small distance for purposes of jumping up one step or overcoming small obstacles. Smaller rovers have been also proposed for planetary exploration, such as NASA-JPL

Nanorover [2] and ESA *NanoKhod* [16]. Both rovers can articulate the main body of the robot, to position it against a rock, or the terrain, with a desired angle. They are capable of self-righting and can carry a minimal scientific instrumentation. Two models of jumping robots used in space exploration are documented in the literature: the first one is the movable vehicle *PROP-F* [17], [18] for the study of Phobos surface, developed by the former Soviet Union, and the second one is the Japanese *Minerva*, developed to explore the surface of asteroid 1998SSF36 during mission MUSES-C [19-25]. In the late 1990's, NASA started a small exploratory program on hopping robots that produced three generations of devices capable of moving by hopping in combination with other locomotion methods. The three generations are shown in the family portrait of Figure 1.

Figure 1. Family portrait of NASA hopping rovers.

Design concepts similar to the Nanokhod [2] have been proposed in [29] as mobility studies and some preliminary analysis of their performance in flight has been presented. However, none of the prototypes and concepts described above addresses in a definitive way the survivability of the robot after a crash landing. The polycarbonate shell of the generation one NASA-JPL hopper is an example of passive protection, and the same is for the crash cage of the generation two prototype. A possible approach consists of using re-inflatable air bags of the *dead-beat* type [27], [28], as proposed in [29]. More recently, the Canadian Space Agency has developed a new design of a hopping robot powered by a cylindrical spring, capable of horizontal jumps up to 2.5 m, and weighting less than 2 Kg [30]. Landing protection is achieved by protecting the hopper with folding solar panels, similar to NASA-JPL generation two prototype, as shown in Figure 2.

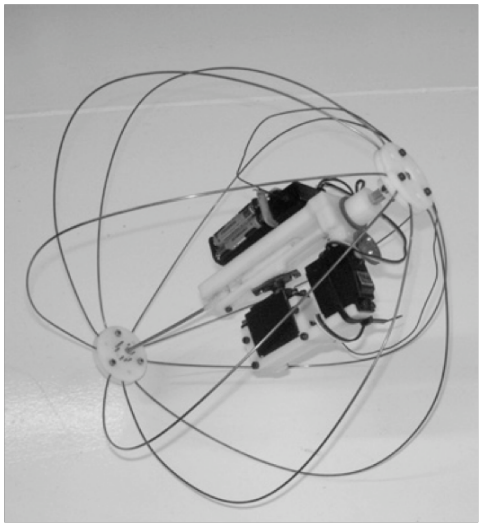

Figure 3: the JollBot

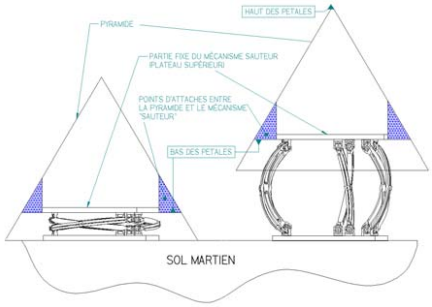

Figure 2: Mechanical configuration of the Canadian Hopping Robot.

CONCEPTS OF LANDING MECHANISM

The design presented in this paper, although developed independently, is similar to the robot JollBot described in [31] as an example of biological inspiration to mobility, and shown in Figure 3. Unlike the JollBot, the concept hopper under development achieves the two main goals of a planetary exploration robot, namely excellent mobility and landing protection, as shown in the artist rendering of Figure 4.

Its main body consists of an elastic cage composed of multiple bended metal strips arranged as the ribs of a Chinese lantern. To jump, the cage is compressed along the vertical axis, properly oriented and suddenly released. The peculiarity of our design is a small foot and a large head: a small foot allows choosing the take off angle at jumping, so that the optimal parabolic trajectory can be approached; a large head will allow carrying a large payload, will protect its inner parts, and will allow an efficient jump since most of the robot mass is concentrated in the head. However, the body orientation at take off need to avoid the contact between the blades and the ground, because it could reduce the jump efficiency. The elastic metal strips of the cage can partially absorb the impact energy at landing, thus achieving the desired landing protection. This design permit also to have a significant design flexibility, since many parameters can be tuned with respect to number, material, length, cross section area, bending profile and linkages of the metal strips, as it is shown in the following preliminary analysis. Figure 4 shows a concept design in which hopping mobility is integrated with legs for self righting capability, precision motions in the vicinity of the target, and orientation setting at take off.

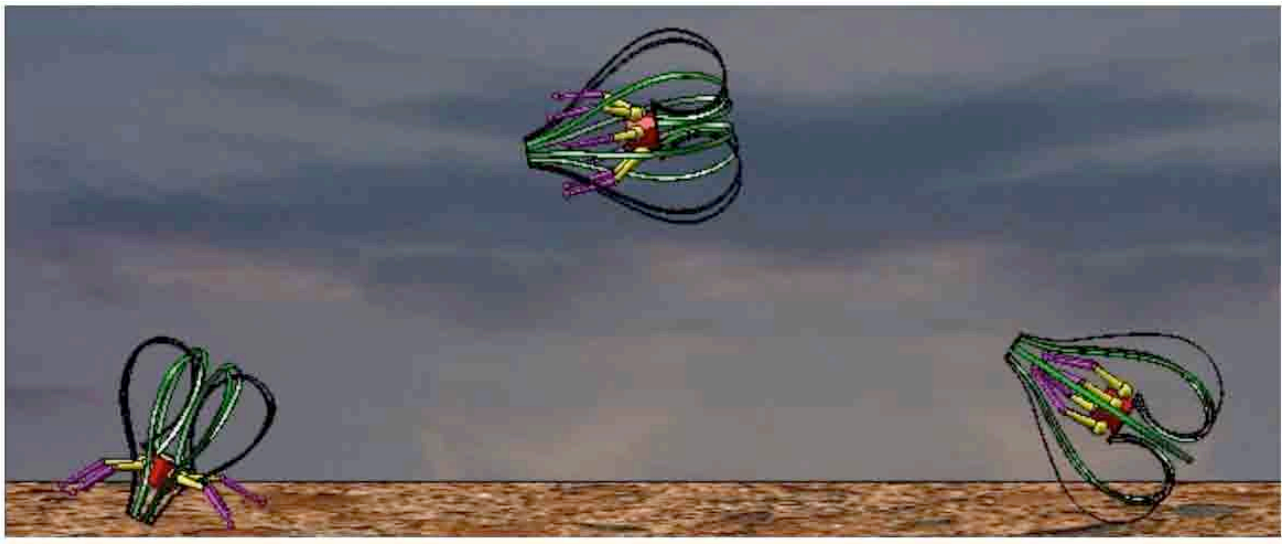

Figure 4: Concept operation of the proposed hopping robot.

PRELIMINARY PROOF OF CONCEPT

The theoretical computation of the optimal set of parameters is a challenging problem and a preliminary experimental study was a good starting point to quickly obtain simple results to compare with the state of the art of jumping robots. We built the first prototype composed of eight strips of harmonic steel, symmetrically welded to two octagonal plates, as shown in Figure 5. Each spring is bent in a bow shape and it consists of one steel blade 510 mm of length, 10 mm of width and 1 mm thick, bent before being welded to the plates. In the uncompressed state the clearance between two parallel plates is 330 mm, the maximum diameter of the cage is about 300 mm, whereas its height is 365 mm. In the full compressed state the clearance is about 100 mm, the maximum diameter is about 420 mm, and the height is about 140 mm. The mass of the complete cage is 0.480 kg, and a payload of 0.770 kg was added to simulate the additional mechanism and scientific payload. To measure the hopper performance in this configuration, we set up a test bench equipped with an ATI FT mini 45 force-torque sensor. With this design, a vertical force of 190 N was applied to compress the cage, and acceleration the forces were measured during take off. The best height achieved was about 1.5 m for vertical jumps. The discharging plot of one of the test run is shown in Figure 6.

Figure 5: Elastic cage design

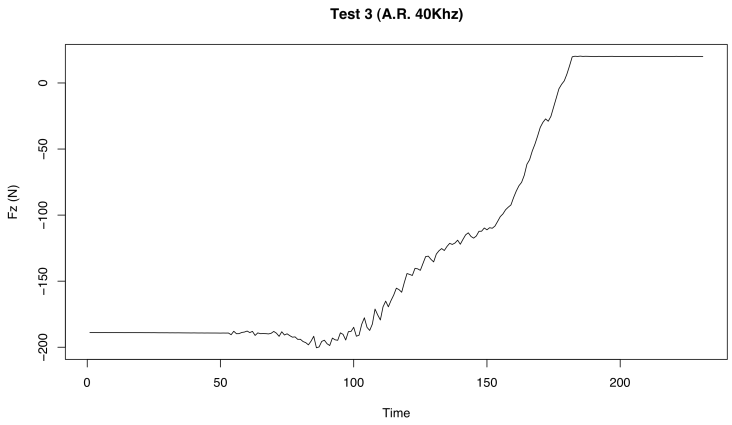

Figure 6: Discharging plot at take off

As demonstrated in [32], one of the key issues in hopping robot design is the capability of generating a force profile at take off that tends to zero when the spring is fully extended. This feature avoids the slippage of the robot when the spring is almost fully extended, due to the reduction of friction with the ground. Thus, some effort has gone into the analysis of the proper spring profile capable of ensuring the desired force delivery curve.

THEORETICAL ANALYSIS

The elastic system is composed by very elastic lamellar curved beams and therefore the large displacement theory has to be used. A special non-incremental finite element was used [33] able to solve the dynamics of the studied system. The local differential equilibrium equations, for a three dimensional beam, describing the dynamics of a slice of a curved beam, have the well-known expressions:

$$\begin{aligned} \frac{\partial}{\partial t}\left(\mathbf{m}\frac{\partial \boldsymbol{u}}{\partial t}\right) &= \frac{\partial \boldsymbol{R}}{\partial s} + \boldsymbol{p} \\ \frac{\partial}{\partial t}\left(\mathbf{J}\omega\right) &= \frac{\partial \boldsymbol{M}}{\partial s} + \nu \times \boldsymbol{R} + \boldsymbol{m} \end{aligned} \tag{1}$$

where $\boldsymbol{u}$ is the displacement vector, containing the three translations along the three axes of the global reference frame; $\boldsymbol{\omega}$ is the angular velocity vector, including the three components of the angular velocity, about the whole axes; matrices **m** and **J** include the mass and the moment of inertia components: in the principal reference frame they have the following expressions:

$$\cdot\ \mathbf{m} = \rho A\begin{bmatrix}1 & 0 & 0\\ 0 & 1 & 0\\ 0 & 0 & 1\end{bmatrix} \qquad \mathbf{J} = \begin{bmatrix}J_1 & 0 & 0\\ 0 & J_2 & 0\\ 0 & 0 & J_3\end{bmatrix} \tag{2}$$

In above equations (1) and (2): *s* is the curvilinear coordinate of the beam centreline, $\boldsymbol{\nu}$ is the unit vector, perpendicular to the local cross-section of the beam, $\boldsymbol{R}$ and $\boldsymbol{M}$ are, respectively, the resultant force and bending moment of stresses acting on the beam cross-section (cohesion forces), while $\boldsymbol{p}$ and $\boldsymbol{m}$ are respectively the distributed force and the distributed moment vectors acting along the axis of the beam. In equation (1), vectors $\boldsymbol{R}$, $\boldsymbol{M}$, $\boldsymbol{p}$ and $\boldsymbol{m}$ are expressed in the global reference frame x,y,z.

If the Timoshenko's beam model is used to describe the mechanical behaviour of the whole system, the cohesion forces $\boldsymbol{R}$ and $\boldsymbol{M}$ are linked to strains by the following relations (Hooke's law) written in the local reference frame X,Y,Z attached to the local cross section:

$$\boldsymbol{R} = \mathbf{D}_0\varepsilon \qquad \boldsymbol{M} = \mathbf{D}\left(\chi - \chi_0\right) = \mathbf{D}\Delta\chi \tag{3}$$

where:

$$\boldsymbol{p}=\begin{Bmatrix}p_1\\p_2\\p_3\end{Bmatrix}\qquad \boldsymbol{m}=\begin{Bmatrix}m_1\\m_2\\m_3\end{Bmatrix}\qquad \boldsymbol{R}=\begin{Bmatrix}N\\Q_2\\Q_3\end{Bmatrix}\qquad \boldsymbol{M}=\begin{Bmatrix}M_t\\M_2\\M_3\end{Bmatrix}\qquad \varepsilon=\begin{Bmatrix}\varepsilon_0\\\vartheta_2\\\vartheta_3\end{Bmatrix}\qquad \chi=\begin{Bmatrix}\chi_t\\\chi_2\\\chi_3\end{Bmatrix} \tag{4}$$

while χ_0 is the initial curvature vector of the undeformed shape of the beam. Subscripts 1, 2, 3 refer to the local reference frame axes: axis 1 is perpendicular to the cross-section, while axes 2 and 3 are the central principal axes of the local cross section. N is the axial effort, namely it should listed as Q_1, but actually in the literature it is referred to as N; Q_2 and Q_3 are shear efforts, M_t is the torque, while M_2 and M_3 are the two bending moments. Matrices $\mathbf{D}_0$ and $\mathbf{D}$ are respectively:

$$\mathbf{D}_0=\begin{bmatrix}EA & 0 & 0\\0 & GA_2 & 0\\0 & 0 & GA_3\end{bmatrix}\qquad \mathbf{D}=\begin{bmatrix}GI_t & 0 & 0\\0 & EI_2 & 0\\0 & 0 & EI_3\end{bmatrix} \tag{5}$$

where in a more general case A_2 and A_3 are the shear areas of the cross section; I_t, I_2 and I_3 are the second order geometrical moments of the cross section and G, E are the transversal and longitudinal elasticity moduli. Vector $\boldsymbol{\varepsilon}$ includes: ε_0, axial deformation of the beam measured at its centreline, ϑ_2 and ϑ_3, the small shear angles between the plane normal to the centreline and the two principal axes of the cross-section, Figures 7-8. Vector $\boldsymbol{\chi}$ contains, χ_t,χ_2 and χ_3, which are torsion angle and curvatures, i.e. the variation of angles between two local reference frames located at the infinitesimal distance ds.

By replacing relations (2) in equations (1) it holds:

$$\begin{aligned}&\frac{\partial}{\partial t}\left(\mathbf{m}\frac{\partial \boldsymbol{u}}{\partial t}\right)=\frac{\partial\left(\mathbf{D}_0\varepsilon\right)}{\partial s}+\chi\times\left(\mathbf{D}_0\varepsilon\right)+\boldsymbol{p}\\&\frac{\partial\left(\mathbf{J}\omega\right)}{\partial t}=\frac{\partial\left(\mathbf{D}\Delta\chi\right)}{\partial s}+\chi\times\left(\boldsymbol{D}\,\Delta\chi\right)+\nu\times\left(\mathbf{D}_0\varepsilon\right)+\boldsymbol{m}-\omega\times\left(\mathbf{J}\omega\right)\end{aligned} \tag{6}$$

System (6) is a set of six equations allowing finding the six displacements, three translations and three rotations.

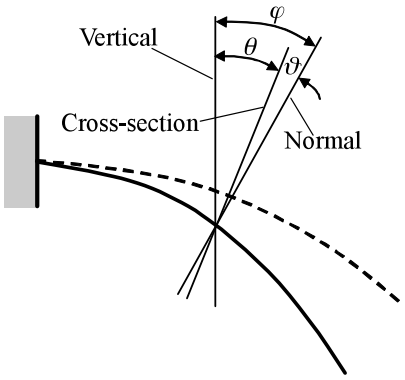

Figure 7: Angle notation

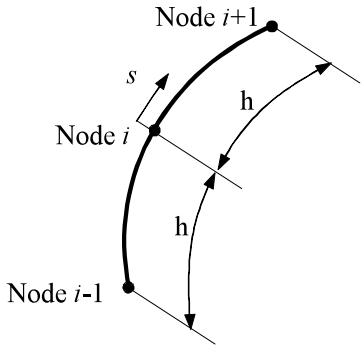

Figure 8: Three-node finite element

For a planae system, i.e. a 2D beam, equations (6) become simpler:

$$\begin{aligned}&\frac{\partial}{\partial t}\left(\mathbf{m}\frac{\partial \boldsymbol{u}}{\partial t}\right)=\frac{\partial\left(\mathbf{D}_0\varepsilon\right)}{\partial s}+\begin{Bmatrix}-GA_2\vartheta_2\chi_3\\EA\varepsilon_0\chi_3\end{Bmatrix}+\boldsymbol{p}\\&J_3\frac{\partial^2\theta}{\partial t^2}=\frac{\partial}{\partial s}\left(EI_3\left(\frac{\partial\theta}{\partial s}-\frac{\partial\theta_0}{\partial s}\right)\right)+GA_2\vartheta_2+m_3\end{aligned} \tag{7}$$

In this case the system includes three equations: two force equilibrium conditions and the moment equilibrium condition. The actual curvature χ_3 and the curvature rate $\Delta\chi$ can be expressed in function of the rotation angle θ of the cross-section:

$$\chi_3=\frac{d\theta}{ds}\qquad \Delta\chi=\frac{d\theta}{ds}-\frac{d\theta_0}{ds} \tag{8}$$

where θ_0 represents the slope of the initially undeformed shape of the beam.

Nonlinear equations (6) and (7) are written for the deformed beam configuration: they are valid even for large displacement, so large that the initial configuration may be completely changed. In this work only the static behaviour was examined, the dynamic analysis will be presented in a future work. For static analysis equations (7) become:

$$\begin{aligned} &\frac{d\left(\mathbf{D}_0\varepsilon\right)}{ds}+\begin{Bmatrix}-GA_2\vartheta_2\chi_3\\ EA\varepsilon_0\chi_3\end{Bmatrix}+\boldsymbol{p}=0\\ &\frac{\partial}{ds}\left(EI_3\left(\frac{\partial\theta}{\partial d}-\frac{\partial\theta_0}{ds}\right)\right)+GA_2\vartheta_2+m_3=0\end{aligned} \tag{9}$$

Often the axial and shearing efforts can be neglected with negligible errors:

$$\frac{\partial}{ds}\left(EI_3\left(\frac{\partial\theta}{\partial d}-\frac{\partial\theta_0}{ds}\right)\right)+m_3=0 \tag{9}$$

This results in an equation with only one unknown describing the large displacement behaviour of elastic beam systems. Based on this theory a curved iso-parametric three-node finite element with only one degree of freedom per node (rotation θ) was elaborated [33].

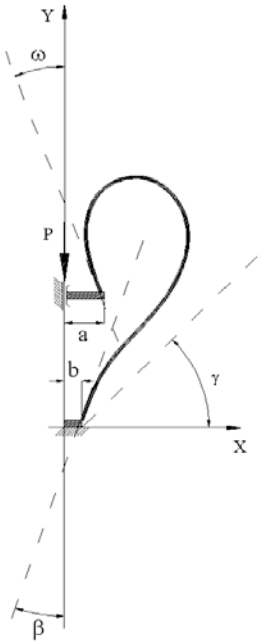

Figure 9: Model used for spring analysis

The configuration of the hopper spring can be modeled as shown in Figure 7, where for example L = 500 mm, width=10 mm, thickness = 1mm, and a = 52 mm, b = 23 mm, ω = -40°, β = 16°. The computation is carried out using the method described above with 101 nodes and 100 elements, and the results are shown in Figure 8.

Figure 10 shows one of the static loading curve of the simulated spring, which achieves the desired configuration.

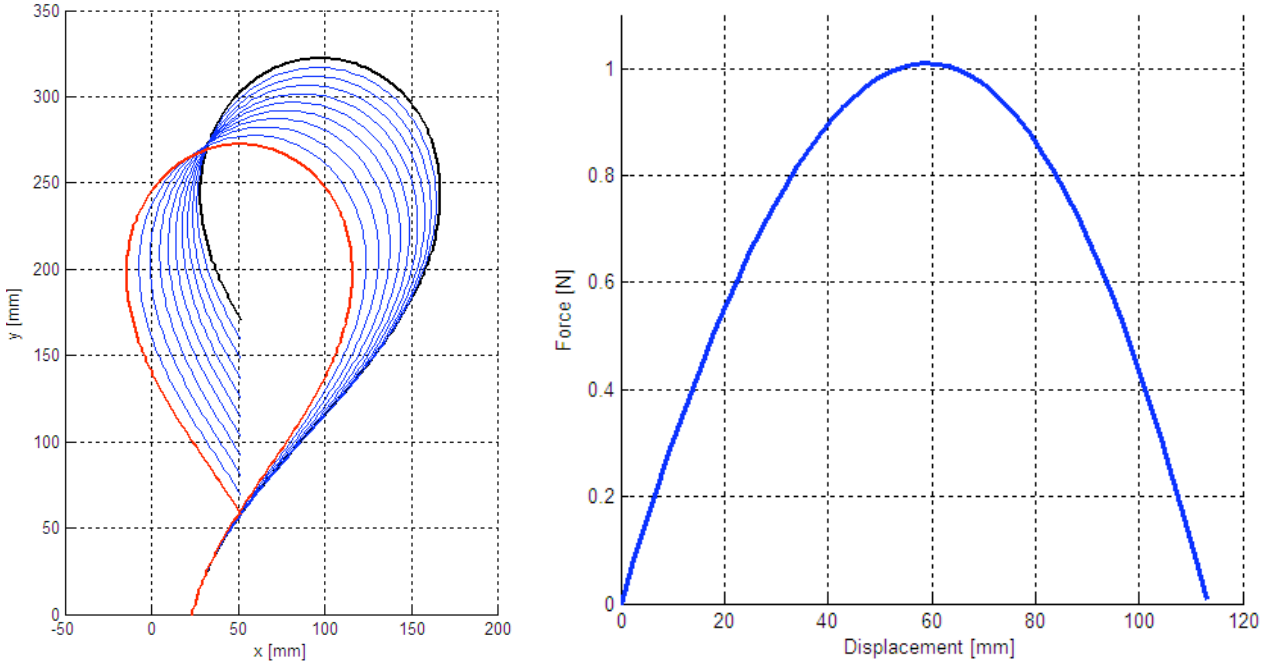

a) b)

Figure 10: Example of spring deflection

CONCLUSIONS

This paper summarizes the research carried out at the University of Verona, in the area of jumping robots for planetary exploration. After reviewing the state of the art of the hopping robot technology, we present a new concept design based on a combined new propulsion/landing protection system with interesting features.
The design consists of an elastic cage capable of impressing several hundred N of force at take off, and protecting the internal instruments at landing. We addressed the study of this concept by combining laboratory experiments with theoretical analysis and simulation. The experiments were in good match with the theoretical results, thus confirming the correctness of the analysis. To get a first idea of the effect of the various parameters on the force delivery profile, we run a set of test with various dimensions, sizes and pre-shapes of the springs, obtaining curves that achieve the desired shape. However to be able to carry out realistic simulations, we are in the process to develop a mathematical model of the propulsion system, so that we can design and fabricate a more performing prototype.

REFERENCES

[1] A. Mishkin and J. Morrison and T. Nguyen and H. Stone and B. Cooper, "Operations and Autonomy of the Mars Pathfinder Microrover", IEEE Aerospace Conf., 1998.
[2] R. Welch and B. Wilcox and A. Nasif, “Nanorover for Mars”, Space Technology, pp 163-172, April 1998, Vol. 17, N. 3-4.
[3] Bares, J. and Hebert, M. and Kanade, T. and Krotkov, K. and Mitchell, T. and Simmons, R. and Whittaker, W., “Ambler: An autonomous rover for planetary exploration", IEEE Computer, pp 18-26, August 1989, Vol. 22, N. 6.
[4] Bares, J. and Wettergreen, D., Dante ii: Technical description, results, and lessons learned, Int. J. of Robotics Research, pp 621-649, July 1999, Vol. 18, N. 7.
[5] Raibert, Marc H, "Legged Robots that Balance", The MIT Press, Cambridge, MA, 1986
[6] J. Oberth , "The Moon Car", Harper and Brothers, New York, 1959
[7] Seifert, H.S., The Lunar Pogo Stick, Journal of Spacecraft and Rockets, pp 941-943, July 1967, Vol. 4, N. 7
[8] Kaplan, M.H. and Seifert, H., "Hopping Transporters for Lunar Exploration", J. Spacecraft and Rockets, pp 917-922, Aug. 1969, Vol. 6, N. 8.
[9] Lorigo, L., Paul, C., Brooks, R.,McLurkin, J. and Moy, M., "Autonomy for Mars Exploration", Workshop on Planetary Rovers at IROS'97, September 7-11, 1997, Grenoble, FR
[10] Zubrin B. et al., Mars gashopper, Pioneer Astronautics, NASA Contract NAS3-00074.
[11] R. C. Johnson, "Hopping robots mark a leap for engineering", EE Times, November 2000, Number 1140:102.

[12] Koditschek D.E. and Bühler, M., "Analysis of a Simplified Hopping Robot", Int. J. Robotics Research, pp 587-605, Dec.1991, Vol. 10, N. 6.
[13] Li, Z. and Montgomery, R., "Dynamics and Optimal Control of a Legged Roboti in Flight Phase", IEEE Int. Conf. on Robotics and Automation, pp 1816-1821, May 1990, Cincinnati, OH.
[14] M'Closkey R.T. and Burdick, J.W., "Periodic motion of a hopping robot with vertical and forward motion", Int. J. Robotics Reseach, pp 197-218, May 1993, Vol. 12, N. 3.
[15] M. D. Berkemeier and R. S. Fearing, "Sliding and hopping gaits for the underactuated acrobot.", IEEE Tansaction on Robotics and Automation, 1998, Vol. 14, N. 4, pp 629-634.
[16] Benjaafar S., Bonney J.C., Budenske J.R., Dvorak M., Gini M., French H., Krantz D.G., Li P.Y., Malver F., Nelson B., Papanikolopoulos N., Rybski P.E., Stoeter S.A., Voyles R and Yesin, K.B., "A miniature robotic system for reconnaissance and surveillance, IEEE Int. Conf. on Robotics and Automation, pp 501-507, May 2000, San Francisco, CA
[17] Siegwart, R., \url{http://asl.epfl.ch/research/systems/Nanokhod/nanokhod.php
[18] Kemurdzhian A. L., Bogomolov A. F., Brodskii P. N., Gromov V. V., Dolginov Sh. Sh., Kirnozov F. F., Kozlov G. V., Komissarov V. I., Ksanfomality L. V., Kucherenko V. I., Martynov B. N., Mishkinyuk V. K., Mitskevich A. V., Rogovskii G. N., Sologub, P. S., Surkov Yu. A., and Turobinskii A. V., "Study of Phobos' Surface with a Movable Robot", International Workshop: Phobos - Scientific and Methodological Aspects of the Phobos Study, pp 357-367, November 24-28 1986, Space Research Institute, USSR Academy of Sciences (1988), Moscow (Russia).
[19] Kemurdzhian, A. L., Brodskii, P. N., Gromov V. V., Kozlov G. V., Komissarov V. I., Kucherenko, V. I., Martynov B. N., Mishkinyuk V. K., Mitskevich A. V., Rogovskii G. N., Sologub P. S., and Turobinskii A. V., Balebanov, V. M., "A Roving Vehicle for Studying the Surface of Phobos (PROP)", Instrumentation and Methods for Space Exploration", pp 136-141, 1989, Nauka Publisher, (In Russian), Moscow (Russia)
[20] Yoshimitsu T, Kubota T., Nakatani I, Kawaguchi, J., "Robotic Lander {MINERVA}, its Mobility and Surface Exploration", Spaceflight Mechanics 2001, Advances in the Astronautical Sciences, pp 491-501, Vol. 108, N. 1, 2001
[21] Yoshimitsu T., Kubota T, Nakatani I,. Adachi T., Saito, H., "Analysis on Hopping Mecanism of Planetary Robotic Vehicle by Microgravity Experiments", Microgravity Sci. Technol, Z-Tec Publishing, Bremen, pp 3-13, 2002, Vol. XIII, N. 4.
[22] Yoshimitsu T., Kubota T., Nakatani I, Adachi T,. and Saito, H., "Micro-hopping robot for asteroid exploration", Acta Astronautica, Pergamon - Elsevier Science Ltd., pp 441-446, 2003, Vol. 52.
[23] Yoshimitsu T, Kubota T,. Nakatani I., "Micro hopping robot for asteroid exploration", IAA Int. Conf. on Low Cost Planetary Missions, pp 1104-1111, 2000,
[24] Yoshimitsu T., Kubota T., Nakatani I., "Analysis on Hopping Mechanism by Microgravity Experiments", Drop Tower Days 2000 in Bremen, pp 63-67, October 9-12, 2000,
[25] Yoshimitsu T., Kubota T., Nakatani I, Adachi T., and Saito, H., "Microgravity Experiment of Hopping Rover", IEEE Int. Conference on Robotics and Automation, pp 2692-2697, October 1999, Detroit (MI-USA).
[26] Yoshimitsu T., Kubota T., Nakatani I., Adachi T., Saito, H., "Hopping Rover "MINERVA" for Asteroid Exploration", Fifth Int. Symp. on artificial Intelligence, Robotics and Automation in Space, pp 83-88, June 1-3 1999.
[27] Dave Northey, Personal communication, May, 2004.
[28] Northey, D. and Morgan, C., "Improved Inflatable Landing System for Low Cost Planetary Landers", IAA Conference, 2003.
[29] Fiorini , P. and Marchesi, M., "Robustness concepts for hopping robots", ASTRA 2004.
[30] Dupuis E., Montminy S., Farhat M., Champliaud H., "Mechanical Design of a Hopper Robot for Planetary Exploration", ASTRA 2006
[31] Armour R., Paskins K., Bowyer A., Vincent J. and Megill W., "Jumping robots: a biomimetic solution to locomotion across rough terrain", Bioinsp. Biomim. 2 (2007) S65–S82
[32] Burdick J. and Fiorini P. "Minimalist Jumping Robots for Celestial Exploration". The International Journal of Robotics Research, Vol. 22, Number 7-8, pp. 653-674, August 2003. Sage Publishers.
[33] Munteanu, M.Gh. and Brusa, E., "Non-linear Dynamic Analysis of Electrostatic Microbeam Actuators", Proc. of Int. Conf. on Computational Methods for Coupled Problems in Science and Engineering, (ECCOMAS conference), Santorini, 25-27 May **2005**,17 pag. (published in extenso on CD).